

# Behaviour of Bi-axially Bent Long H-Piles

by

K. Kurma Rao\*

M.R. Madhav\*\*

## Introduction

During a pile testing program at the site of Ontario Hydro's new Lambton Generating Station, Hanna (1968) observed large deflections, while driving, about the weak axis of H-section piles. Similar cases were also reported by Bjerrum (1957). There are instances in which two piles formed a conjunctive ( $U$ ) so that one rose while the other was driven down and vice-versa (1968). The deviation of the pile axis from vertical can be measured by the use of inclinometer. In case of H-steel piles, a square duct is formed for inclinometer readings, by tack welding an angle to the web and one flange of H-pile. When inclinometer measurements are required in case of precast concrete piles, a steel pipe, say of 40 mm diameter, is cast concentrically in the pile. The load on such an initially deformed pile will no longer be axial, and bending moments occur in the pile section. In addition to the moment in the pile section, the distortion of the pile material, the cumulative effect of bending, residual, and axial stresses leads to an appreciable decrease of the load carrying capacity.

The usual limit on allowable distortion of the pile axis is two per cent of the length of the pile. From extensive tests in Norway, Bjerrum (1957) stated that any driven H-section pile with a radius of curvature of less than 400m is rejected. However, Hanna (1968) reported a very small bending radius of about 60m in his investigation. It is shown in this investigation that a rational solution for finding the limiting radius of curvature is possible. The pile is idealised as a beam and the soil by a Winkler medium characterised by the modulus of subgrade reaction. Three different end conditions are considered as shown in Fig. 1.

## Idealization

The governing differential equation representing the force system on a bent pile with constant moment of inertia, (Johnson et al. 1968) is represented as :

$$EI \frac{d^4 u_2}{dy^4} + P \cdot \frac{d^2 u_2}{dy^2} + kD u_2 = - P \frac{d^2 u_1}{dy^2} \quad \dots(1)$$

where  $u_2$  is additional deflection of pile under  $p$  and  $u_1$ ,  $E$ ,  $k$ ,  $D$  are initial shape (deflection) of the pile, Young's modulus of the pile material, foundation modulus and diameter of the pile respectively. Equation 1 is

---

\* Professor, College of Engineering, Kakinada, (AP), India.

\*\* Professor, Indian Institute of Technology, Kanpur, 208016, India.

(The revised paper was received in January, 1986 and is open for discussion till the end of September, 1986)

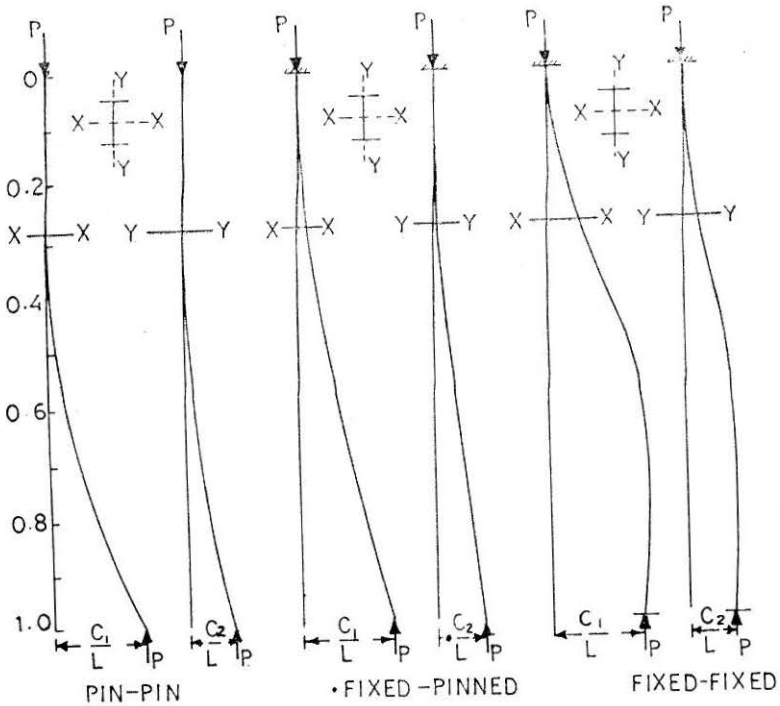


FIGURE 1 Pile Boundary Conditions Considered (a) Pinned-Pinned  
(b) Fixed-Pinned (c) Fixed-Fixed

applicable to any smooth and uniformly bent end-bearing pile irrespective of the pile boundary conditions. It is assumed in Eq. (1) that the lateral earth pressure is linearly related to the pile deflection. The axial force as well as soil modulus are assumed to be invariant with depth. Equation (1) may be non-dimensionalized by substituting,

$$w_2 = \frac{u_2}{L}; Z = \frac{y}{L}; \text{ and } w_1 = \frac{u_1}{L} \quad \dots(2)$$

where  $L$  is the length of the pile. Substituting Eq. (2) and their derivatives in Eq. (1), a non-dimensionalized equation is obtained as follows :

$$\frac{d^4 w_2}{dz^4} + \alpha_1 \frac{d^2 w_2}{dz^2} + \alpha_2 w_2 = -\alpha_1 \frac{d^2 w_1}{dz^2} \quad \dots(3)$$

where  $\alpha_1 = \frac{PL^2}{EI}$  and  $\alpha_2 = \frac{KD}{EI} \cdot L^4$

Mixed end conditions such as a fixed head and a pinned tip are common. The fixed non-translating boundary condition at either end is also of interest in pile foundations. End bearing pile with hinged end conditions is quite common and was dealt by Marcus and is reported by Johnson et al. (19:8). In dimensionless form, the initial shape for fixed-fixed

boundary conditions, may be represented as :

$$w_1 = \frac{1}{2\pi} \frac{C}{L} [1 + 2\pi z - \cos 2\pi z - \sin 2\pi z] \quad \dots(4)$$

where  $C$  is the offset of the pile tip from vertical axis. Equation (4) satisfies both natural and geometric boundary conditions as follows :

$$\begin{aligned} \text{when } z = 0, w_1 = 0; \frac{dw_1}{dz} = 0; \frac{d^2 w_1}{dz^2} \neq 0 \text{ and } \frac{d^3 w_1}{dz^3} \neq 0 \\ \text{and when } z = 1.0, w_1 = \frac{C}{L}; \frac{dw_1}{dz} = 0; \frac{d^2 w_1}{dz^2} \neq 0 \text{ and } \frac{d^3 w_1}{dz^3} \neq 0 \end{aligned} \quad \dots(5)$$

Let the particular solution of Eq. (3) for fixed-fixed boundary conditions be

$$w_3' = F (\sin 2\pi z + \cos 2\pi z) \quad \dots(6)$$

where  $w_2'$  is the additional deflection of the pile under load  $P$ . Substituting Eqs. (4) and (6) and their derivatives in Eq. (3) and comparing like terms the following relation can be obtained.

$$F = - \frac{2\pi\alpha_1}{(16\pi^4 - 4\pi^2 + \alpha_2)} \cdot \frac{C}{L} \quad \dots(7)$$

The solution for homogeneous part of Eq. (3) is

$$\begin{aligned} w_2'' = C_1 \cdot \sin(m_1 z) \cdot \cosh(m_2 z) + C_2 \cos(m_1 z) \cdot \sinh(m_2 z) \\ + D_1 \sin(m_1 z) \cdot \sinh(m_2 z) + D_2 \cos(m_1 z) \cdot \cosh(m_2 z) \end{aligned} \quad \dots(8)$$

where  $C_1$ ,  $C_2$ ,  $D_1$  and  $D_2$  are constants to be determined by boundary conditions and  $m_1^2 = \sqrt{\frac{\alpha_2}{4} + \frac{\alpha_1}{4}}$  and  $m_2^2 = \sqrt{\frac{\alpha_2}{4} - \frac{\alpha_1}{4}}$ . Substituting four boundary conditions stated in Eq. (5) the constants  $C_1$ ,  $C_2$ ,  $D_1$  and  $D_2$  can be evaluated.

The total additional deflection under load  $P$  is

$$w_2 = w_2' + w_2'' \quad \dots(9)$$

When the load  $P$  attains critical value, the additional deflection  $w_2'$  should theoretically be large and therefore  $F$  in Eq. (7) should become infinitely great. This is possible when

$$16\pi^4 - 4\pi^2 \alpha_1 + \alpha_2 = 0$$

$$\text{Therefore } P_{cr} = \frac{4 EI}{\pi^2 L^2} [16\pi^4 + \frac{kD}{EI} \cdot L^4] \quad \dots(10)$$

Similarly the initial shape for fixed-pinned boundary conditions may be represented as :

$$w_1 = \frac{C}{L} \left(1 - \cos \frac{\pi z}{2}\right) \quad \dots(11)$$

The critical load for fixed-pinned boundary conditions may be represented likewise by :

$$P_{cr} = \frac{4 EI}{\pi^2 L^2} \left[ \frac{\pi^4}{16} + \frac{kD}{EI} L^4 \right] \quad \dots(12)$$

### Bi-axially Bent Piles

The sectional properties of H-pile considered are given in Table 1. Figure 1 shows the assumed shapes of the pile about both the axes for different conditions. The deflections out of the vertical about the weak axis have been reported to be large compared to those about the strong axis (Hanna, 1968). When the H-section shown in Fig. 2, bends along  $X-X$  and in the direction of arrow shown perpendicular to it, maximum compressive stresses occur at  $A$  and  $B$  and maximum tensile stresses at  $C$  and  $D$ . Similarly when bending takes place along the strong axis  $y-y$ , compressive stresses at  $B$  and  $D$  and tensile stresses at  $A$  and  $C$ , are induced. Consequently, maximum stresses occur at edges  $B$  and  $C$ . In case of bi-axially bent H-pile, residual stresses due to initial bending about both the axes, bending stresses due to load  $P$  about both axes and the axial stress, occur and they are cumulative.

TABLE 1  
Sectional Properties of H-Pile

Size cm	Wt/metre Kg.	Depth $D$ cm	Width $B$ cm	Area <sub>2</sub> cm	$I_{xx}$ cm <sup>4</sup>	$I_{yy}$ cm <sup>4</sup>
35.56 × 36.83	53.07	36.15	37.8	221.56	1864.6	5114.5

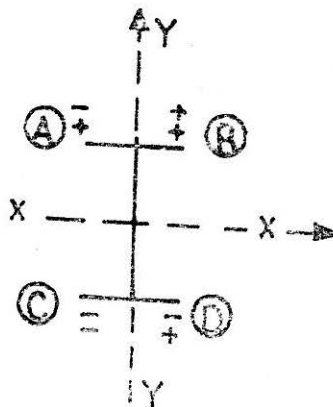


FIGURE 2 Section of Steel Pile

For fixed-fixed boundary conditions the expression for stresses are presented herein. Residual stresses may be represented by :

$$S_1 = -2\pi \frac{C_1}{L} (\sin 2\pi z + \cos 2\pi z)$$

$$S_2 = -2\pi \frac{C_2}{L} (\sin 2\pi z + \cos 2\pi z)$$

where  $S_1$  and  $S_2$  are the residual stresses,  $C_1$  and  $C_2$  are the pile offsets along the weak and strong axes respectively. The flexural stress,  $S_3$ , along the weak axis may be represented as :

$$\begin{aligned} S_3 = & 4\pi^2 F_1 (\sin 2\pi z + \cos 2\pi z) - \sin m_1 h \cdot \sinh m_2 z [D_1 (m_2^2 - m_1^2) \\ & - 2D_2 m_1 m_2] - \cos m_1 z \cdot \cosh m_2 z [D_2 (m_2^2 - m_1^2) + 2D_1 m_1 m_2] \\ & - \sin m_1 z \cdot \cosh m_2 z [C_1 (m_2^2 - m_1^2) - 2C_2 m_1 m_2] \\ & - \cos m_1 z \cdot \sinh m_2 z [C_2 (m_2^2 - m_1^2) + 2C_1 m_1 m_2] \end{aligned}$$

$$\text{where } F_1 = - \frac{2\pi \alpha_1}{(16x^4 - 4\pi^2 \alpha_1 + \alpha_2)} \cdot \frac{C_1}{L}$$

A similar expression for stress,  $S_4$ , along the strong axis under the load  $P$  can be obtained. The expressions  $S_1$  through  $S_4$  are obtained making use of the general elastic-flexure equation for beams.

Axial stress  $S_5$  equals the axial load divided by the cross-sectional area of the H-pile. The total stress in a bent pile should be limited to  $S$ , the ultimate or working stress as the case may be, of the pile material, that is

$$\frac{S_1 + S_2 + S_3 + S_4 + S_5}{S} = 1.0 \quad \dots(13)$$

Equation (13) is solved using iterative procedure until the values are within an error of  $\pm 0.0001$ . Similar expressions are obtained for pinned-pinned and fixed-fixed boundary conditions.

Once the radii of curvature  $R_1$  and  $R_2$  along the weak and strong axes under load  $P$  are known, it is always advantageous to find the equivalent radius of curvature,  $R_e$ , expressed as  $R_e = \frac{R_1 R_2}{R_1 + R_2}$  ... (14)

## Results and Discussion

Based on the results obtained from the analysis, percentage load carrying capacity of a bent pile as a ratio of the capacity of a straight one is plotted against non-dimensionalized pile off-set. Figures 3 and 4 represent such relationships for pinned-pinned, fixed-fixed and fixed-hinged boundary conditions. The curves are drawn for off-sets upto 5 percent along the weak axis and 2 percent along the strong axis. Numerical results are

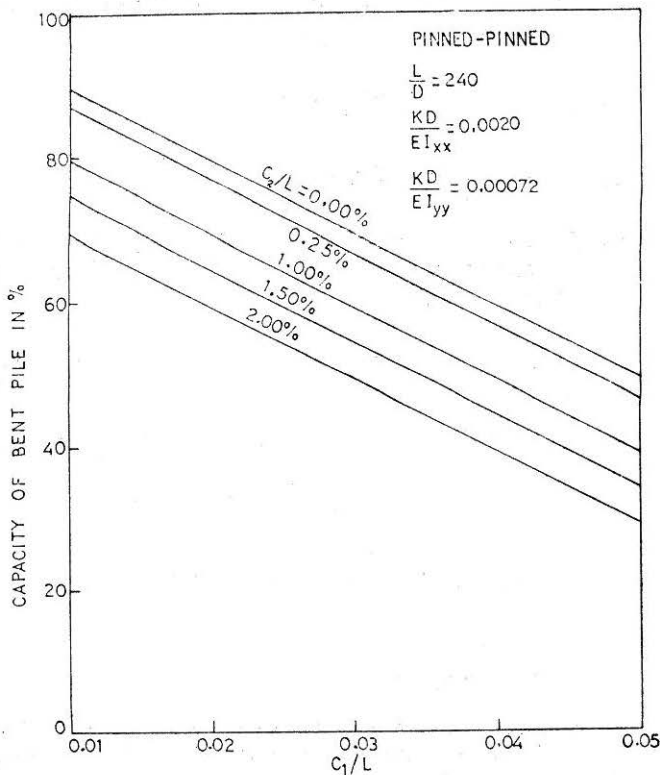


FIGURE 3 Effect of Pile Off-Set on Capacity of Bent Pile Pinned-Pinned Case.

obtained for  $\frac{L}{D} = 240$ ;  $\frac{kD}{EI_{xx}} = 0.0020$ ;  $\frac{kD}{EI_{yy}} = 0.00072$  and for various combinations of pile off-sets along both the axes. The variation of load carrying capacity is linear with respect to the pile off-sets in case of pinned-pinned and fixed-pinned boundary conditions whereas it appears to be parabolic in case of fixed-fixed boundary conditions. Figure 5 shows the effect of slenderness ratio on the percentage load carrying capacity of a bent pile. The results are illustrated for 1 percent of pile off-set along the strong axis. From Figs 3 through 5, for a given pile off-set along the weak axis and a known slenderness ratio, it is observed that the percentage load carrying capacity of a bent pile is maximum for fixed-fixed boundary conditions. For example, from Fig. 5, for slenderness ratio of 200 and 2 percent off-set along the weak axis, the percentage load carrying capacities of fixed-pinned, pinned-pinned and fixed-fixed boundary conditions are 81, 63 and 38.5 per cent respectively. It is also observed that the load carrying capacity of a bent pile for given pile off-set, increases with increase of slenderness ratio. This is due to the fact that the residual stresses, which are of considerable magnitude in bent piles, are inversely proportional to the slenderness ratio. It may be concluded that long piles can sustain greater pile off-sets.

In Fig. 6, the ratio of  $R_e$  and  $D$  is plotted against percentage load carrying capacity of bent pile. For steel pile the material reaches yield

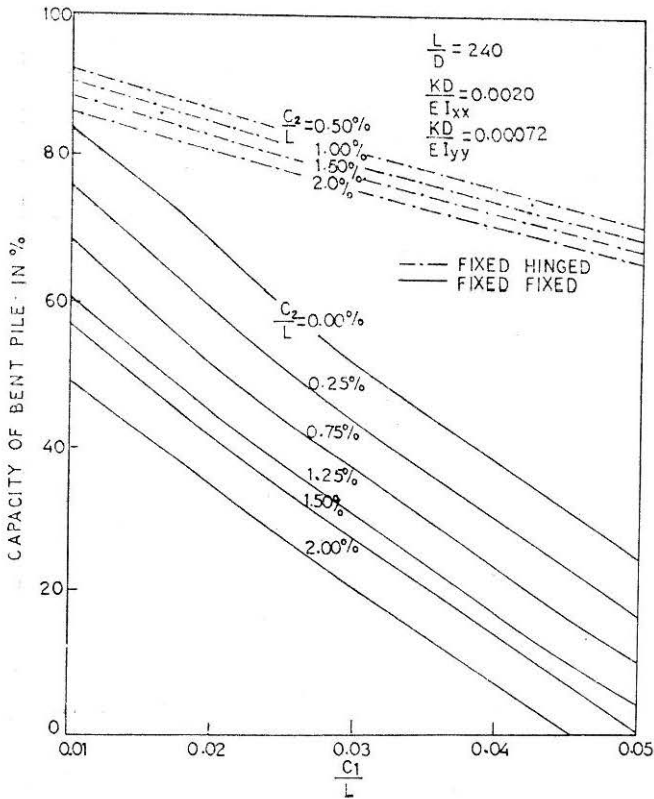


FIGURE 4 Effect of Pile Off-Set on Capacity of Bent Pile  
(a) Fixed-Hinged (b) Fixed-Fixed.

stress when the ratio of  $R_e$  to depth of flange,  $D$ , reached 400. This is the limiting value. When the ratio  $R_e/D$  falls below this limiting value, the pile cannot take any load. In Fig. 6, it can be seen that as the ratio increases from the limiting value, the curve becomes asymptotic to cent percent load carrying capacity line. According to Bjerrum (1957), the Norwegian authorities reject H-section piles if bending radius is smaller than 400m. For a H-section of depth of 30 cm, such a pile can bear as much as 60.0 percent of the load carrying capacity of a straight pile.

Initially bent piles, do bend further under load. However, the change in radius of curvature is comparatively small for larger off-sets. Table 2 illustrates the changes in the ratio of  $R_e/D$  for a pile of slenderness ratio 80 and for different pile off-sets under ultimate load. The initial equivalent radius of curvature can be calculated once the initial shapes of the pile along both the axes are known. Since the change in radius of curvature under load will not be substantial, the approximate load carrying capacity of a bent pile can be calculated from Fig. 6 based on the initial equivalent radius of curvature. The error in the solution may be of the order of 3 to 4 percent only.

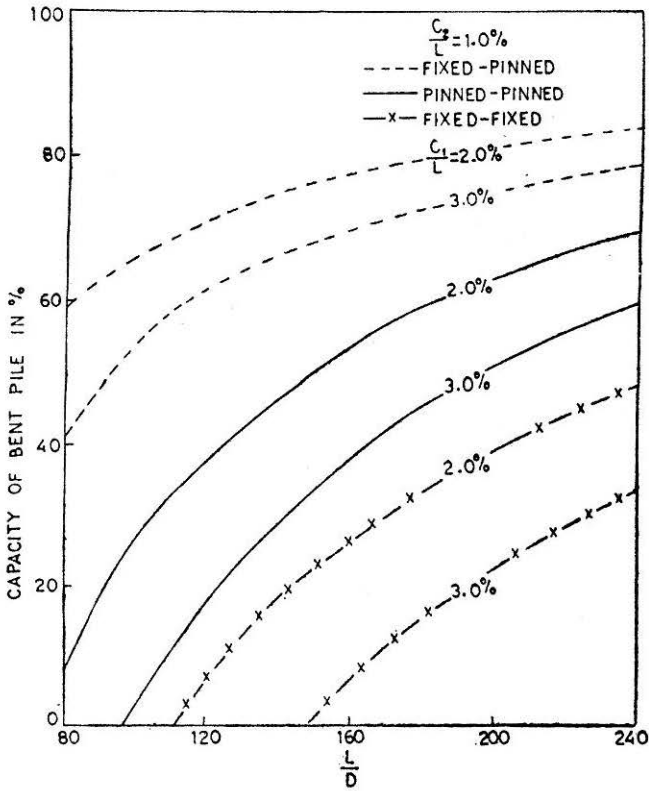


FIGURE 5 Effect of Slenderness Ratio on Capacity of Bent Pile

TABTE 2

Increase of Radius of Curvature Under Load

$\frac{C}{L}$	$\frac{PL^3}{EI}$	Minimum Radius of Curvature $R_0/D$ (Non-dimensionalized)	
		Initial Equivalent Curvature	Equivalent Radius of Curvature Under Load
0.0100	91.4162	1766	1566
0.0200	72.5731	1148	1041
0.0300	55.5581	850	789
0.0400	39.9232	678	641



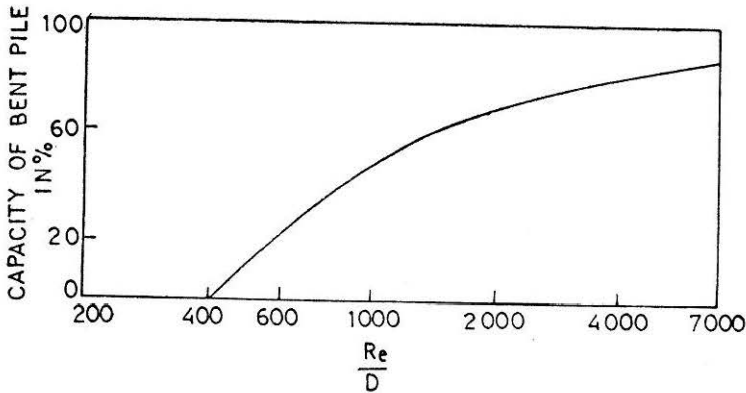


**FIGURE 6** Relationship Between Radius of Curvature (Non-Dimensionalized) and Load Carrying Capacity of Bent Pile

### Conclusions

The behaviour of bi-axially bent long H-piles has been studied for three boundary conditions. For known pile off-sets along both the axes, and a given slenderness ratio, fixed-pinned boundary conditions take maximum load when compared with pinned-pinned and fixed-fixed conditions. For given ratio of pile off-set and length, the load carrying capacity of a bent pile increases with increasing slenderness ratio. The material in the H-pile may attain yield stress when the ratio of  $R_e$  and  $D$  attains value of 400. Once the initial shape is known, the approximate estimate of the load carrying capacity of the pile can be made directly using Fig. 6 of the present investigation.

### Notations

The following symbols are used in this paper:

- $C_1, C_2$  = coefficients,
- $c_1$  = pile off-set along weak axis,
- $c_2$  = pile off-set along strong axis,
- $D$  = depth of H-pile along web direction,
- $D_1, D_2$  = coefficients,
- $EI$  = flexural rigidity of the pile in the plane of bending,
- $F, F_1$  = coefficients,
- $k$  = soil modulus
- $L$  = length of pile,
- $m_1, m_2$  = characteristic roots,
- $P$  = axial load,
- $P_{cr}$  = buckling load,
- $R_1$  = radius of curvature along the weak axis,

- $R_2$  = radius of curvature along the strong axis,  
 $R_e$  = equivalent radius of curvature,  
 $S_1$  = residual stress along weak axis,  
 $S_2$  = residual stress along strong axis,  
 $S_3$  = flexural stress along weak axis under load  $P$ ,  
 $S_4$  = flexural stress along strong axis under load  $P$ ,  
 $S_5$  = axial stress under load  $P$ ,  
 $u_1$  = initial deflection of the pile,  
 $u_2$  = additional deflection of the pile,  
 $w_1$  = non-dimensionalized initial deflection of the pile,  
 $w_2$  = non-dimensionalized additional deflection of the pile,  
 $Z$  = non-dimensionalized pile length,  
 $\alpha_1$  =  $PL^2/EI$   
 $\alpha_2$  =  $kD L^4/EI$

### References

- BJERRUM, L. (1957): "Norwegian Experience with Steel Piles to Rock", *Geotechnique* 7: 73-76.
- HANNA, T.H., (1968) : "The Bending of Long-H-Section Piles" *Canadian Geotechnical Journal*, 5; 150-172.
- JOHNSON, S.M., and KAVANAGH, T.C., (1968): "*The Design of Foundations for Buildings*, McGraw-Hill Book Co., Inc., New York.